Theoretical performance of near-field conventional beamforming by using linear array sonar

WANG Wen-sheng[1], YANG Xiu-ting[2]

(1. *Dalian Neusoft Institute of Information, Dalian* 116023, *Liaoning, China*;
2. *Department of Operational Commands, the Navel Academy of PLA, Dalian* 116018, *Liaoning, China*)

Abstract: The performance of passive localization via conventional beamforming (CBF) by using uniform linear array has been investigated in this paper. In order to locate the noisy underwater target-the heavy thermal powered torpedoes usually confronted in anti-submarine war (ASW), the asymptotic estimate error of CBF is analyzed and compared with the Cramer-Rao bound (CRB) to show the passive localization performance, thereafter, the factors such as the signal strength, target location, array aperture and observation time have also been investigated via numerical simulations. The results show that the middle-range passive localization of torpedoes can be probably solved by using the existing SONAR equipment (such as flank array SONAR).

Key words: linear array sonar; passive localization; beamforming

1　INTRODUCTION

CBF is one of the most important signal processing methods to acquire the spatial gain for improving the signal to noise ratio (SNR) in the modern sonar systems. By using CBF, Sonar has the ability not only to detect the underwater weak signal imbedded in background noise, but to locate the weak target as well. In the ASW scenarios, the incoming torpedo should be detected at sufficient range for effective countermeasure. Moreover, it is usually important to estimate the range of incoming torpedo for accurate deployment of acoustic jammers and decoys, therefore the near-field (NF) wave model should be adopted to replace the plane-wave assumption.

As well known, passive localization forms a conventional difficulty in the underwater acoustic engineering[1], and only near-field ranging is feasible. In the near-field scenario, time delay between the hydrophones is different from that of the plane-wave field (which only depends on the bearing of target), and it can be expressed as a function of target's bearing and the distance from the target to the receiving array[2]. Therefore, the time delay should be compensated both in the bearing and distance dimension when the beamforming technique is used.

In recent years, the flank array sonar has grown into popular equipment used by the conventional and nuclear submarines for long range detection due to its large aperture. In order to reduce the system complexity and decrease the number of sonar systems, it seems a valuable idea to integrate the passive ranging function (which is done by the passive ranging sonar) with the flank-array sonar. Some primary research has been reported in the near past years[3].

In this paper, the two dimensional estimation of bearing and range by using the uniform linear flank-array sonar has been investigated via near-field beamforming (NF-CBF). The estimation performance of NF-CBF is demonstrated by the asymptotic estimate error, and compared with the Cramer-Rao lower bound. The numerical results show that it is possible for the flank-array sonar to provide acceptable passive ranging accuracy for the tactical use of soft-skill weapons.

2　THEORETICALLY MODELING FOR NF-CBF

2.1　Steering vector of NF-CBF

As shown in Fig. 1, the ULA with M elements each spaced by d is receiving the acoustic signal radiated by a near-field acoustic target. Choosing the first hydrophone as the origin, the position of
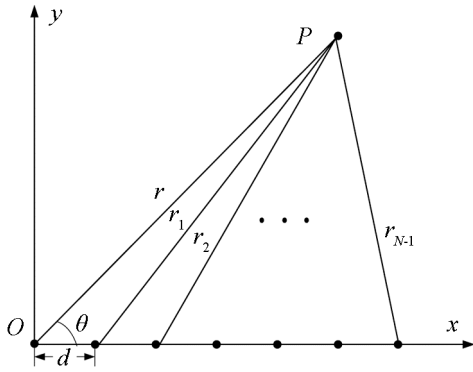
Fig.1　The geometric structure of near-field bemforming

target can be denoted as (r, θ), and the acoustic distance from the target to each hydrophone can be written as

$$r_m=\sqrt{r^2+x_m^2-2rx_m\cos\theta}\quad(m=1,\cdots,M)\qquad(1)$$

Where x_m is the x-coordinate component of the m-th hydrophone, given by

$$x_m=(m-1)d\qquad(2)$$

In the near-field scenario, when $r\Box(M-1)d$, i.e. the range of target is much greater than the sonar's aperture, Equation (1) can be expanded in a Taylor series. Neglecting the terms with second order above, we have

$$r_m\approx r\left(1-\frac{x_m\cos\theta}{r}+\frac{x_m^2\sin^2\theta}{2r^2}\right)\qquad(3)$$

By using Equation (1) and (3), we obtain the difference of the acoustic distance between the first and the m-th hydrophones

$$\Delta r_m=r-r_m\approx x_m\cos\theta-\frac{x_m^2\sin^2\theta}{2r}\qquad(4)$$

Then the associated propagation time delay is

$$\Delta\tau_m=\frac{\Delta r_m}{c}\approx\frac{x_m\cos\theta}{c}-\frac{x_m^2\sin^2\theta}{2rc}\qquad(5)$$

For the narrowband beamformer with a central frequency of f, the steering vector of the ULA can be written as

$$a(r,\theta)=\left[1,e^{jh_1},\cdots,e^{jh_{M-1}}\right]^T\qquad(6)$$

Where "T" denotes transpose manipulation. h_m ($m=1,\cdots,M-1$) is determined by

$$h_m=\frac{2\pi md\cos\theta}{\lambda}-\frac{\pi m^2d^2\sin^2\theta}{r\lambda}\qquad(7)$$

Equation (6) can also be written

$$a(r,\theta)=a_1(\theta)\Box\ a_2(r,\theta)\qquad(8)$$

Where "$\Box$" denotes the Schur-Hadamard product. The vector s of $a_1(\theta)$ and $a_2(r,\theta)$ are given

$$a_1(\theta)=\left[1,e^{j\frac{2\pi d\cos\theta}{\lambda}},\cdots,e^{j\frac{2\pi(M-1)d\cos\theta}{\lambda}}\right]^T\qquad(9a)$$

$$a_2(r,\theta)=\left[1,e^{-j\frac{\pi d^2\sin^2\theta}{r\lambda}},\cdots,e^{-j\frac{\pi(M-1)^2d^2\sin^2\theta}{r\lambda}}\right]^T\qquad(9b)$$

Where $a_1(\theta)$ only depends on the target's bearing, *i. e.* a steering vector according to the plane wave acoustic field, $a_2(r,\theta)$ considers the cylindrical spreading caused by the near-field effect, and the target's distance can be estimated by phase compensation in this vector. In the following text, we use a, a_1 and a_2 to denote these three vectors mentioned above for convenience.

From Equation (3), neglecting the term with second order, yields

$$r_m\approx r\left(1-\frac{x_m\cos\theta}{r}\right)\qquad(10)$$

It is easily known that the steering vector based on Equation (10) is that demonstrated in Equation (9a)，so we can see that the assumption of plane wave neglects all the terms higher than second order.

2.2　Data model of receiving array

In the near-field scenario, when there exist J sources, the output of the M-ray ULA can be written as

$$x(t)=A(\vartheta)s(t)+n(t)\qquad(11)$$

Where the vectors of received data, noise and signal at instant t can be given by

$$x(t)=[x_1(t),\cdots,x_M(t)]^T$$
$$n(t)=[n_1(t),\cdots,n_M(t)]^T$$
$$s(t)=[s_1(t),\cdots,s_J(t)]^T$$

$A(\vartheta)$ (expressed by **A** in the following) denotes the manifold of ULA, given by

$$\mathbf{A}=\left[a(\vartheta_1),\cdots,a(\vartheta_J)\right]^T\qquad(12)$$

Where the parameter vector of multi-target is written as $\vartheta=[\vartheta_1,\cdots,\vartheta_J]^T$, and the position parameter vector of the j-th target is

$$\vartheta_j=\left[r_j,\theta_j\right]^T,\ (j=1,\cdots,J)\qquad(13)$$

By using the received data, we can simultaneously estimate the bearing and distance of the target via beamforming methods such as CBF.

2.3　Position estimation

The position parameter vector $\vartheta=[r,\theta]^T$ can be estimated by

$$\hat{\vartheta}=\arg\max a^H\mathbf{R}a\qquad(14)$$

Where **R** denotes the covariance matrix of the received array, by using Equation (11), we have

$$R = E\left[x(t)x^H(t)\right] = APA^H + \sigma_n^2 I \qquad (15)$$

Where $P = E\left[s(t)s^H(t)\right]$ denotes the signal co-variance matrix, I is an identity matrix, σ_n^2 is the noise variance.

When multi-targets exist, the position vector can be estimated by

$$\left.\frac{\partial f(\boldsymbol{\vartheta})}{\partial \boldsymbol{\vartheta}}\right|_{\boldsymbol{\vartheta}=\hat{\boldsymbol{\vartheta}}} = 0 , \quad f(\boldsymbol{\vartheta}) = a^H R a \qquad (16)$$

3 PERFORMANCE ANALYSIS OF NF-CBF

The NF-CBF method searches the maximum in the two dimensional field of bearing and range, and estimate the position vector by the output power. The theoretical performance of the NF-CBF will be analyzed in this part. For convenience, the following assumptions should be made:

(1) The noise received by each hydrophone is mutually independent, and can be deemed as a zero-mean Gaussian random process with covariance σ_n^2;

(2) The signal radiated by the target is also a narrowband zero-mean Gaussian process with variance σ_s^2.

(3) The noise and signal is mutually independent.

In the following, both the theoretical and asymptotic performance of the NF-CBF will be deduced.

3.1 Asymptotic analysis

The position vector can be estimated via NF-CBF by using Equation (14). In the realistic signal processing, the maximum likelihood estimate of the data covariance matrix can be given by

$$\hat{R} = \frac{1}{N}\sum_{n=1}^{N} x(n)x^H(n) \qquad (17)$$

Therefore, the position vector of target is estimated by the following relation

$$\left.\frac{\partial \hat{f}(\boldsymbol{\vartheta})}{\partial \boldsymbol{\vartheta}}\right|_{\boldsymbol{\vartheta}=\hat{\boldsymbol{\vartheta}}} = 0 , \quad \hat{f}(\boldsymbol{\vartheta}) = a^H \hat{R} a \qquad (18)$$

The estimate error can be written as

$$\Delta\boldsymbol{\vartheta} = \hat{\boldsymbol{\vartheta}} - \boldsymbol{\vartheta} = \hat{\boldsymbol{\vartheta}} - \bar{\boldsymbol{\vartheta}} + \bar{\boldsymbol{\vartheta}} - \boldsymbol{\vartheta} = \Delta\tilde{\boldsymbol{\vartheta}} + \Delta\bar{\boldsymbol{\vartheta}} \qquad (19)$$

Where $\Delta\tilde{\boldsymbol{\vartheta}} = \hat{\boldsymbol{\vartheta}} - \bar{\boldsymbol{\vartheta}}$ is a random error, and $\Delta\bar{\boldsymbol{\vartheta}} = \bar{\boldsymbol{\vartheta}} - \boldsymbol{\vartheta}$ is the bias difference caused by finite samples.

From Equation (19), for the reason that

$E\Delta\tilde{\boldsymbol{\vartheta}} \approx \mathbf{0}$ [4], then the estimate variance of the position vector is

$$\text{var}(\boldsymbol{\vartheta}) \approx E\Delta\tilde{\boldsymbol{\vartheta}}\Delta\tilde{\boldsymbol{\vartheta}}^T + \Delta\bar{\boldsymbol{\vartheta}}\Delta\bar{\boldsymbol{\vartheta}}^T \qquad (20)$$

According to [4], the two terms in the right side of Equation (20) can be written as

$$E\Delta\tilde{\boldsymbol{\vartheta}}\Delta\tilde{\boldsymbol{\vartheta}}^T = \left\{\text{Re}\left[D^H RD + H\right]\right\}^{-1} \cdot$$
$$\frac{a^H Ra\,\text{Re}\left[D^H RD\right] - D^H Ra a^H RD}{2N} \cdot \qquad (21)$$
$$\left\{\text{Re}\left[D^H RD + H\right]\right\}^{-1}$$

$$\Delta\bar{\boldsymbol{\vartheta}}\Delta\bar{\boldsymbol{\vartheta}}^T \approx \left\{\text{Re}\left[D^H RD + H\right]\right\}^{-1} \cdot$$
$$\text{Re}\left[D^H Ra\right]\text{Re}\left[\left(D^H Ra\right)^T\right] \cdot \qquad (22)$$
$$\left\{\text{Re}\left[D^H RD + H\right]\right\}^{-1}$$

In Equation (21) and (22), the matrix D and H are defined as

$$D = \left[\frac{\partial a}{\partial r}, \frac{\partial a}{\partial \theta}\right] \qquad (23)$$

$$H = \begin{bmatrix} a^H R\dfrac{\partial^2 a}{\partial r^2} & a^H R\dfrac{\partial^2 a}{\partial r \partial \theta} \\[2mm] a^H R\dfrac{\partial^2 a}{\partial r \partial \theta} & a^H R\dfrac{\partial^2 a}{\partial \theta^2} \end{bmatrix} \qquad (24)$$

When the asymptotic condition is satisfied, we have

$$\left.\frac{\partial f(\bar{\boldsymbol{\vartheta}})}{\partial \boldsymbol{\vartheta}}\right|_{\bar{\boldsymbol{\vartheta}} \to \boldsymbol{\vartheta}} = 2\text{Re}\left[D^H Ra\right] = 0 \qquad (25)$$

Substituting Equation (25) into Equation (22), yields

$$\Delta\bar{\boldsymbol{\vartheta}}\Delta\bar{\boldsymbol{\vartheta}}^T \approx 0 \qquad (26)$$

Therefore, from Equation (20), we have

$$\text{var}(\boldsymbol{\vartheta}) \approx E\Delta\tilde{\boldsymbol{\vartheta}}\Delta\tilde{\boldsymbol{\vartheta}}^T \qquad (27)$$

3.2 The Cramer-Rao lower bound

In multi-target scenario, when the parameters such as position vector $\boldsymbol{\vartheta}$, signal matrix P and noise variance σ_n^2 are all unknown, the Cramer-Rao lower bound of the $\boldsymbol{\vartheta}$ can be given by[5]

$$\text{CRB}(\boldsymbol{\vartheta}) = \frac{\sigma_n^2}{2N}\left\{\text{Re}\left[(U \otimes l_2)\square\left(D^H P_A^\perp D\right)^T\right]\right\}^{-1} \quad (28)$$

Where "$\otimes$" denotes the Kronecker product, N is the number of independent samples.

$$U = P\left(A^H AP + \sigma_n^2 I\right)^{-1} A^H AP \qquad (29a)$$

$$P_A^\perp = I - A\left(A^H A\right)^{-1} A^H \qquad (29b)$$

$$D = \left[\frac{\partial a}{\partial r^{(1)}}, \frac{\partial a}{\partial \theta^{(1)}}, \cdots, \frac{\partial a}{\partial r^{(J)}}, \frac{\partial a}{\partial \theta^{(J)}}\right] \qquad (29c)$$

It should be pointed out that the geometric pattern of the hydrophone array in Equation (29)

can be arbitrary.

4 NUMERICAL RESULTS

In this section, the theoretical analysis mentioned in Section 3 will be carried out by numerical calculations.

Example 1:

Consider a 48-ray ULA with element space of 0.5m for data receiving. The data in single-target scenario is collected with the position vector (4350m, 90°). The central frequency for narrowband processing is f =1500 Hz, and totally 10 independent snapshots are used.

Fig. 2 shows the range and bearing variance with the increase of SNR respectively. From the figures we can see that both the asymptotic variance and Cramer-Rao lower bound are much greater in the range estimation than those in the bearing estimation. It forms a challenging task for the passive sonar to provide feasible ranging accuracy for tactical use. In the narrowband processing, only the middle-range target (with higher signal strength and nearer range) can be estimated with acceptable accuracy. In Fig 2 (a), the asymptotic variance of range at 15dB is about 1200 m, which can provide reluctant target indication for soft-skill deployment. From the results of Fig. 2, we can also draw the conclusion that the estimate accuracy of range can be much improved in passive ranging for noise thermal-power torpedo via broadband processing.

Example 2:

The torpedo is approaching the submarine (equipped with ULA sonar) via back chasing to trajectory from the alarming distance (7000m) 3600m.

Fig. 3 shows the range and bearing history of the incoming torpedo. In this example, the range is changed from 7000m to 3500m, and the bearing is changed from 150° to 90°. As can be seen in quation(22), at the beginning of trajectory, the incoming torpedo is in the lower-accuracy estimation zone of the linear array.

Fig.4 shows the range and bearing estimate of the incoming torpedo with a trajectory depicted in Fig. 3. From Fig. 3 we can see that the range estimate is much more difficult than that of the bearing, but from Fig. 3(a) we see that the accuracy of range is improved dramatically with the decreasing
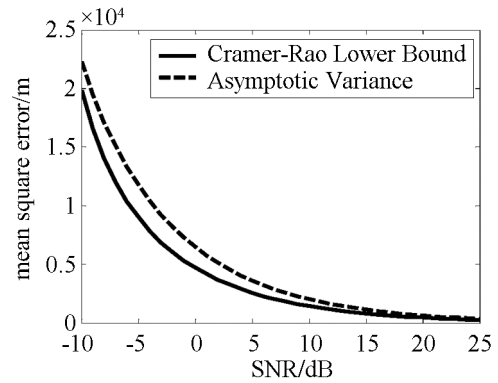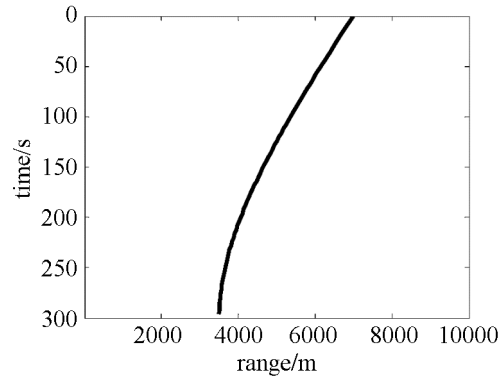

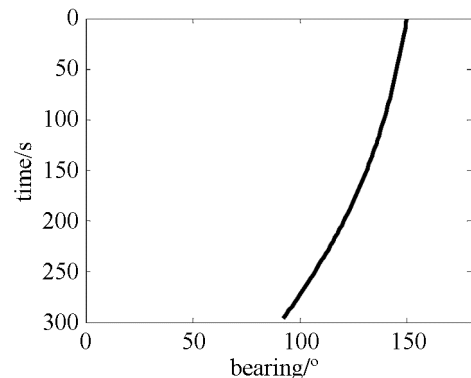(a) Range variance vs. SNR
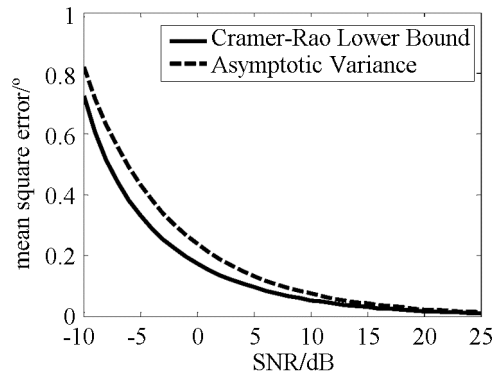
(b) Bearing variance vs. SNR

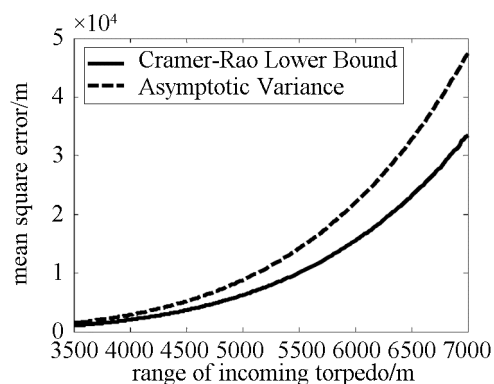Fig.2 Theoretical performance of the NF beamforming

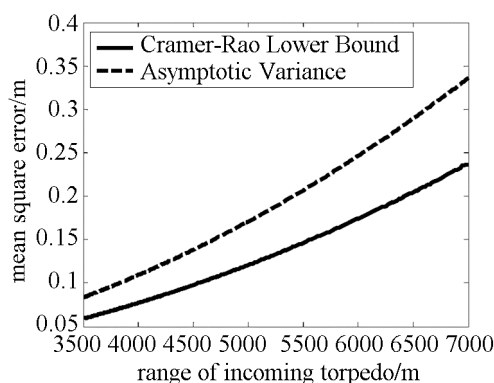(a) Range time record of the torpedo

(b) Bearing time record of the torpedo.

Fig.3 Range and bearing record of the incoming torpedo.

of range, so it is possible to approach the feasible estimate accuracy for providing valuable advice of soft-kill acoustic countermeasure weapon deployments.

(a) Range time record of the torpedo

(b) Bearing time record of the torpedo.

Fig.4   Range and bearing record of the incoming torpedo.

5   CONCLUSIONS

In this paper, the theoretical positioning performance of the NF-CBF algorithm is discussed by using the passive flank-array sonar. The numerical results show that it is possible to estimate the range of the threatening target by using the flank array for effective torpedo countermeasure. Nevertheless, there are some problems still need to be solved for the proper use of flank-array sonar, such as how to estimate the range to achieve a satisfying accuracy by continuous observation and broadband signal processing, and which forms the future work.

References

[1]   LI Qihu. The introduction of sonar signal processing[M]. 2nd edition. Beijing: the Ocean Press. 2000: 334-340.

[2]   ZHENG Zhaoning, XIANG Dawei. The theory of underwater acoustic signal passive detection and parameters estimation[M]. Beijing: Science Press, 1983: 481-488.

[3]   Meister M, Neumeister D. Advanced ranging sonar: passive range measurement with line-arrays[R]. UDT 2006.

[4]   Hawkes M, Nehorai A. Acoustic vector-sensor beamforming and capon direction estimation[J]. IEEE Trans. On Signal Processing, 1998, **46**(9): 2291-2304.

[5]   Nehoari A, Paldi E. Vector-sensor array processing for electro-magnetic source localization[J]. IEEE Trans. on Signal Processing, 1994, **42**(2): 376-398.

线列阵声纳近场常规波束形成的理论性能

王文生[1]，杨秀庭[2]

(1. 大连东软信息学院，辽宁大连　116023；2. 海军大连舰艇学院作战指挥系，辽宁大连　116018)

摘要：研究了线列阵声纳应用常规波束形成方法进行目标被动定位的理论性能。在反潜战中，重型热动力鱼雷是潜艇面临的重要威胁。为对鱼雷实施被动定位，推导了常规波束形成方法目标被动定位的渐进方差，并与克拉美-劳下界进行了比对分析。此外，通过数值方法研究了信号强度、目标位置、基阵孔径和积分时间等参数对被动定位性能的影响。结果表明：应用现有的声纳设备(如潜艇舷侧阵)来解决中等距离的鱼雷被动定位问题是完全可能的。

关键词：线列阵声呐；被动定位；波束形成